

Convergence Rate of Efficient MCMC with Ancillarity-Sufficiency Interweaving Strategy for Panel Data Models

Makoto Nakakita^{1*}, Tomoki Toyabe², Teruo Nakatsuma³, Takahiro Hoshino^{1,3}

¹Center for Advanced Intelligence Project, RIKEN

²Faculty of Economics, Kanazawa Gakuin University

³Faculty of Economics, Keio University
makoto.nakakita@riken.jp,

July 25, 2025

Abstract

Improving Markov chain Monte Carlo algorithm efficiency is essential for enhancing computational speed and inferential accuracy in Bayesian analysis. These improvements can be effectively achieved using the ancillarity–sufficiency interweaving strategy (ASIS), an effective means of achieving such gains. Herein, we provide the first rigorous theoretical justification for applying ASIS in Bayesian hierarchical panel data models. Asymptotic analysis demonstrated that when the product of prior variance of unobserved heterogeneity and cross-sectional sample size N is sufficiently large, the latent individual effects can be sampled almost independently of their global mean. This near-independence accounts for ASIS’s rapid mixing behavior and highlights its suitability for modern “tall” panel datasets. We derived simple inequalities to predict which conventional data augmentation scheme—sufficient augmentation (SA) or ancillary augmentation (AA)—yields faster convergence. By interweaving SA and AA, ASIS achieves optimal geometric rate of convergence and renders the Markov chain for the global mean parameter asymptotically independent and identically distributed. Monte Carlo experiment confirm that this theoretical efficiency ordering holds even for small panels (e.g., $N = 10$). These findings confirm the empirical success of ASIS application across finance, marketing, and sports, laying the groundwork for its extension to models with more complex covariate structures and nonGaussian specifications.

1 Introduction

The scope and applicability of Bayesian panel data analysis have expanded with advancements in Markov chain Monte Carlo (MCMC) methods, particularly the Metropolis–Hastings

*Corresponding author.

algorithm [14, 7] and Gibbs sampler [6]; a comprehensive review on Bayesian panel data analysis is provided by [2].

The data augmentation (DA) algorithm [24] extends the observed dataset by introducing latent variables to handle incomplete data. Since its introduction, DA has formed the basis for various MCMC extensions and continue to evolve in theoretical and applied contexts. A single statistical model within a DA framework can have multiple equivalent formulations. Identifying the most computationally efficient formulation—known as the reparametrization problem—is widely studied in Bayesian hierarchical models [5, 8, 19, 20, 21]. The ancillarity–sufficiency interweaving strategy (ASIS) [27] addresses this challenge by alternating between two parameterizations during sampling, rather than relying on a single formulation. Particularly, ASIS interleaves sufficient augmentation (SA or centered parameterization) and ancillary augmentation (AA or noncentered parameterization). Each scheme exhibits a convergence trade-off: when one converges quickly, the other often slows down [4]. ASIS combines both schemes to achieve superior mixing and convergence than either scheme used alone.

Since its introduction, ASIS has been widely adopted and extended across various domains. Notable early developments include the residual augmentation framework [26], which reinterprets interweaving via residual-based transformations. In financial econometrics, [9] incorporated ASIS into stochastic volatility models, and [10] later generalized it to multivariate factor stochastic volatility models using shallow and deep interweaving schemes. ASIS has also been used for analyzing financial time-series data in recent studies [12, 13, 15, 18, 25].

Despite advances in MCMC techniques, the application of Bayesian hierarchical modeling in panel data frameworks remains underdeveloped. Although ASIS has already been applied in panel data contexts [17, 22, e.g.], a rigorous theoretical foundation for its use is lacking. In addition, strong correlations between random and fixed effects often arise, and treating them as separate blocks can worsen the mixing of the MCMC chain [4]. Herein, we demonstrate that, under certain conditions, ASIS enables the sampling of unobserved heterogeneity α within panel data frameworks almost independently of the global mean μ_α .

Our primary finding is that when the product of the prior variance of unobserved heterogeneity and the sample size must be sufficiently large, latent heterogeneity effectively decouples from the global parameters. In such cases, the ASIS sampler approximates conditional independence and enables faster mixing than either SA or AA alone. This result highlights ASIS’s compatibility with the growing availability of large-scale (“tall”) panel datasets. We also derive approximate conditions—within the conventional panel data framework and for sufficiently large sample sizes—under which one can predict whether SA or AA will converge more rapidly.

2 Convergence Rate of Data Augmentation

Consider two alternative parameterizations of a panel data regression model: SA and AA.

$$\text{(SA)} \quad y_{it} = \alpha_i + \epsilon_{it}, \quad \alpha_i \sim \mathcal{N}(\mu_\alpha, \sigma_\alpha^2), \quad (1)$$

$$\begin{aligned} \text{(AA)} \quad y_{it} &= \mu_\alpha + \tilde{\alpha}_i + \epsilon_{it}, \quad \tilde{\alpha}_i \sim \mathcal{N}(0, \sigma_\alpha^2), \\ \epsilon_{it} &\sim \mathcal{N}(0, \sigma_\epsilon^2), \quad i = 1, \dots, N, \quad t = 1, \dots, T, \end{aligned} \quad (2)$$

A regression function $x_{it}^\top \beta$, where x_{it} is a vector of explanatory variables and β is the corresponding coefficient vector, can be incorporated into equations (1) or (2) by redefining y_{it} as $y_{it} - x_{it}^\top \beta$.

where y_{it} denotes the observation for Individual i at a time t , α_i represents the individual-specific mean of y_{it} , and $\tilde{\alpha}_i$ is the deviation of α_i from the global mean (hyperparameter) μ_α .

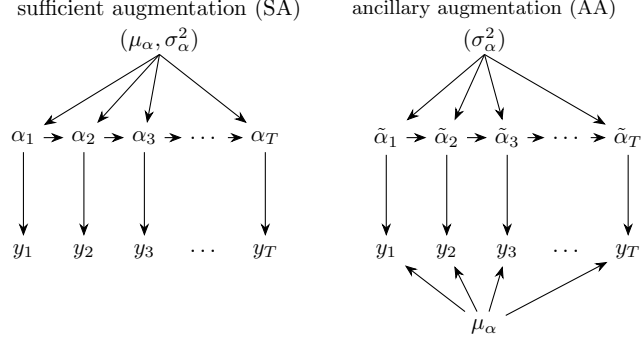


Figure 1: Comparison of parameter dependence between sufficient augmentation (SA) and ancillary augmentation (AA).

Suppose the prior distribution of μ_α is $\mathcal{N}(\varphi_\alpha, \tau_\alpha^2)$, and σ_ϵ^2 and σ_α^2 are known.

Let $\mathcal{D} = (y_{11}, \dots, y_{NT})$ denote the observed data, $\alpha = (\alpha_1, \dots, \alpha_N)$ denote the vector of individual-specific effects, and $\tilde{\alpha} = (\tilde{\alpha}_1, \dots, \tilde{\alpha}_N)$ denote the vector of deviations from the global mean. The Gibbs sampling algorithm under each parameterization is then derived as follows.

(SA)

$$\alpha_i | \mu_\alpha, \mathcal{D} \sim \mathcal{N} \left(\frac{\sigma_\epsilon^{-2} \sum_{t=1}^T y_{it} + \sigma_\alpha^{-2} \mu_\alpha}{\lambda_\alpha}, \frac{1}{\lambda_\alpha} \right), \quad (3)$$

$$\mu_\alpha | \alpha, \mathcal{D} \sim \mathcal{N} \left(\frac{\sigma_\alpha^{-2} \sum_{i=1}^N \alpha_i + \tau_\alpha^{-2} \varphi_\alpha}{\lambda_{\mu SA}}, \frac{1}{\lambda_{\mu SA}} \right), \quad (4)$$

(AA)

$$\tilde{\alpha}_i | \mu_\alpha, \mathcal{D} \sim \mathcal{N} \left(\frac{\sigma_\epsilon^{-2} \sum_{t=1}^T (y_{it} - \mu_\alpha)}{\lambda_\alpha}, \frac{1}{\lambda_\alpha} \right), \quad (5)$$

$$\mu_\alpha | \tilde{\alpha}, \mathcal{D} \sim \mathcal{N} \left(\frac{\sigma_\epsilon^{-2} \sum_{i=1}^N \sum_{t=1}^T (y_{it} - \tilde{\alpha}_i) + \tau_\alpha^{-2} \varphi_\alpha}{\lambda_{\mu AA}}, \frac{1}{\lambda_{\mu AA}} \right), \quad (6)$$

$$\lambda_\alpha = \sigma_\epsilon^{-2} T + \sigma_\alpha^{-2}, \quad \lambda_{\mu SA} = \sigma_\alpha^{-2} N + \tau_\alpha^{-2}, \quad \lambda_{\mu AA} = \sigma_\epsilon^{-2} NT + \tau_\alpha^{-2}.$$

Introduce $z_0, z_1, \dots, z_N \sim \mathcal{N}(0, 1)$. Then, (3) and (4) are equivalent to

$$\alpha_i = \frac{\sigma_\epsilon^{-2} \sum_{t=1}^T y_{it} + \sigma_\alpha^{-2} \mu_\alpha}{\lambda_\alpha} + \frac{z_i}{\sqrt{\lambda_\alpha}}, \quad i = 1, \dots, N, \quad (7)$$

$$\mu_\alpha = \frac{\sigma_\alpha^{-2} \sum_{i=1}^N \alpha_i + \tau_\alpha^{-2} \varphi_\alpha}{\lambda_{\mu SA}} + \frac{z_0}{\sqrt{\lambda_{\mu SA}}}, \quad (8)$$

respectively. Similarly, equations (5) and (6) can be rearranged as follows:

$$\tilde{\alpha}_i = \frac{\sigma_\epsilon^{-2} \sum_{t=1}^T (y_{it} - \mu_\alpha)}{\lambda_\alpha} + \frac{z_i}{\sqrt{\lambda_\alpha}}, \quad i = 1, \dots, N, \quad (9)$$

$$\mu_\alpha = \frac{\sigma_\epsilon^{-2} \sum_{i=1}^N \sum_{t=1}^T (y_{it} - \tilde{\alpha}_i) + \tau_\alpha^{-2} \varphi_\alpha}{\lambda_{\mu AA}} + \frac{z_0}{\sqrt{\lambda_{\mu AA}}}. \quad (10)$$

The Markov process for μ_α in the Gibbs sampler under the SA parameterization is then derived from equations (7) and (8) as follows:

$$\begin{aligned} \mu_\alpha^{(r+1)} &= \frac{\sigma_\alpha^{-2}}{\lambda_{\mu SA}} \sum_{i=1}^N \left(\frac{\sigma_\epsilon^{-2} \sum_{t=1}^T y_{it} + \sigma_\alpha^{-2} \mu_\alpha^{(r)}}{\lambda_\alpha} + \frac{z_i}{\sqrt{\lambda_\alpha}} \right) + \frac{\tau_\alpha^{-2} \varphi_\alpha}{\lambda_{\mu SA}} + \frac{z_0}{\sqrt{\lambda_{\mu SA}}} \\ &= \frac{\sigma_\alpha^{-2}}{\lambda_{\mu SA}} \left(\frac{\sigma_\alpha^{-2} N}{\lambda_\alpha} \mu_\alpha^{(r)} + \frac{\sigma_\epsilon^{-2} \sum_{i=1}^N \sum_{t=1}^T y_{it}}{\lambda_\alpha} + \frac{\sum_{i=1}^N z_i}{\sqrt{\lambda_\alpha}} \right) + \frac{\tau_\alpha^{-2} \varphi_\alpha}{\lambda_{\mu SA}} + \frac{z_0}{\sqrt{\lambda_{\mu SA}}} \\ &= \frac{\sigma_\alpha^{-2}}{\sigma_\alpha^{-2} + \tau_\alpha^{-2}/N} \left(\frac{\sigma_\alpha^{-2}}{\lambda_\alpha} \mu_\alpha^{(r)} + \frac{\sigma_\epsilon^{-2} T \bar{y}_i}{\lambda_\alpha} + \frac{\bar{z}}{\sqrt{\lambda_\alpha}} \right) + \frac{\tau_\alpha^{-2} \varphi_\alpha}{\lambda_{\mu SA}} + \frac{z_0}{\sqrt{\lambda_{\mu SA}}}, \quad r = 1, \dots, R, \end{aligned} \quad (11)$$

where $\bar{y}_i = \frac{1}{NT} \sum_{i=1}^N \sum_{t=1}^T y_{it}$ and $\bar{z} = \frac{1}{N} \sum_{i=1}^N z_i$. Similarly, the Markov process for μ_α in the Gibbs sampler under the AA parameterization is derived from equations (9) and (10) as follows:

$$\begin{aligned} \mu_\alpha^{(r+1)} &= \frac{\sigma_\epsilon^{-2}}{\lambda_{\mu AA}} \sum_{i=1}^N \sum_{t=1}^T \left(y_{it} - \frac{\sigma_\epsilon^{-2} \sum_{t=1}^T (y_{it} - \mu_\alpha^{(r)})}{\lambda_\alpha} - \frac{z_i}{\sqrt{\lambda_\alpha}} \right) + \frac{\tau_\alpha^{-2} \varphi_\alpha}{\lambda_{\mu AA}} + \frac{z_0}{\sqrt{\lambda_{\mu AA}}} \\ &= \frac{\sigma_\epsilon^{-2}}{\lambda_{\mu AA}} \left(\frac{\sigma_\epsilon^{-2} NT^2}{\lambda_\alpha} \mu_\alpha^{(r)} + NT \bar{y}_i - \frac{\sigma_\epsilon^{-2} NT^2 \bar{y}_i}{\lambda_\alpha} - \frac{NT \bar{z}}{\sqrt{\lambda_\alpha}} \right) + \frac{\tau_\alpha^{-2} \varphi_\alpha}{\lambda_{\mu AA}} + \frac{z_0}{\sqrt{\lambda_{\mu AA}}} \\ &= \frac{\sigma_\epsilon^{-2}}{\sigma_\epsilon^{-2} + \tau_\alpha^{-2}/NT} \left(\frac{\sigma_\epsilon^{-2} T}{\lambda_\alpha} \mu_\alpha^{(r)} + \frac{\sigma_\alpha^{-2} \bar{y}_i}{\lambda_\alpha} - \frac{\bar{z}}{\sqrt{\lambda_\alpha}} \right) + \frac{\tau_\alpha^{-2} \varphi_\alpha}{\lambda_{\mu AA}} + \frac{z_0}{\sqrt{\lambda_{\mu AA}}}, \quad r = 1, \dots, R. \end{aligned} \quad (12)$$

When $\tau_\alpha^2 N$ is sufficiently large,

$$\begin{aligned} \frac{\sigma_\alpha^{-2}}{\sigma_\alpha^{-2} + \tau_\alpha^{-2}/N} &\rightarrow 1, \quad \frac{\tau_\alpha^{-2} \varphi_\alpha}{\sigma_\alpha^{-2} N + \tau_\alpha^{-2}} \rightarrow 0, \quad (SA) \\ \frac{\sigma_\epsilon^{-2}}{\sigma_\epsilon^{-2} + \tau_\alpha^{-2}/NT} &\rightarrow 1, \quad \frac{\tau_\alpha^{-2} \varphi_\alpha}{\sigma_\epsilon^{-2} NT + \tau_\alpha^{-2}} \rightarrow 0 \quad (AA). \end{aligned}$$

Thus, as $\tau_\alpha^2 N \rightarrow \infty$, (11) and (12) reduce to

$$\mu_\alpha^{(r+1)} \rightarrow \frac{\sigma_\alpha^{-2}}{\lambda_\alpha} \mu_\alpha^{(r)} + \frac{\sigma_\epsilon^{-2} T \bar{y}_i}{\lambda_\alpha} + \frac{\bar{z}}{\sqrt{\lambda_\alpha}} + \frac{z_0}{\sqrt{\lambda_{\mu SA}}}, \quad (13)$$

$$\mu_\alpha^{(r+1)} \rightarrow \frac{\sigma_\epsilon^{-2} T}{\lambda_\alpha} \mu_\alpha^{(r)} + \frac{\sigma_\alpha^{-2} \bar{y}_i}{\lambda_\alpha} - \frac{\bar{z}}{\sqrt{\lambda_\alpha}} + \frac{z_0}{\sqrt{\lambda_{\mu AA}}}. \quad (14)$$

Theorem 1. *In the approximated Markov processes (13) and (14),*

$$\frac{\sigma_\epsilon^{-2}T}{\sigma_\epsilon^{-2}T + \sigma_\alpha^{-2}} + \frac{\sigma_\alpha^{-2}}{\sigma_\epsilon^{-2}T + \sigma_\alpha^{-2}} = 1. \quad (15)$$

This theorem highlights a fundamental trade-off in convergence behavior: if one algorithm converges rapidly (i.e., exhibits good mixing), the other necessarily converges more slowly (i.e., shows stronger persistence).

Corollary 1. *From Theorem 1, the following trade-off relationship can be easily derived:*

$$\begin{cases} SA \text{ converges faster if } \sigma_\epsilon^2 < \sigma_\alpha^2 T; \\ AA \text{ converges faster if } \sigma_\epsilon^2 > \sigma_\alpha^2 T. \end{cases} \quad (16)$$

This corollary can be directly derived from equation (15). This indicates that the relative convergence rates of SA and AA depend on the length of the time dimension T in the panel data. Although this result is asymptotic, we subsequently demonstrate via simulations that the ordering established in Corollary 1 persists even for small panel datasets, with as few as $N = 10$ individuals.

3 Why ASIS Improves the Convergence Rate

The SA→AA ASIS algorithm is summarized below:

$$\begin{aligned} \alpha_i^{(r+0.5)} &= \frac{\sigma_\epsilon^{-2} \sum_{t=1}^T y_{it} + \sigma_\alpha^{-2} \mu_\alpha^{(r)}}{\lambda_\alpha} + \frac{z_i^{(r+0.5)}}{\sqrt{\lambda_\alpha}}, \\ \mu_\alpha^{(r+0.5)} &= \frac{\sigma_\alpha^{-2} \sum_{i=1}^N \alpha_i^{(r+0.5)} + \tau_\alpha^{-2} \varphi_\alpha}{\lambda_{\mu SA}} + \frac{z_0^{(r+0.5)}}{\sqrt{\lambda_{\mu SA}}}, \\ \tilde{\alpha}_i^{(r+0.5)} &= \alpha_i^{(r+0.5)} - \mu_\alpha^{(r+0.5)}, \\ \mu_\alpha^{(r+1)} &= \frac{\sigma_\epsilon^{-2} \sum_{i=1}^N \sum_{t=1}^T (y_{it} - \tilde{\alpha}_i^{(r+0.5)}) + \tau_\alpha^{-2} \varphi_\alpha}{\lambda_{\mu AA}} + \frac{z_0^{(r+1)}}{\sqrt{\lambda_{\mu AA}}}. \end{aligned} \quad (17)$$

If the approximation in equation (13) holds, then we obtain:

$$\begin{aligned} \tilde{\alpha}_i^{(r+0.5)} &= \alpha_i^{(r+0.5)} - \mu_\alpha^{(r+0.5)} \\ &= \frac{\sigma_\epsilon^{-2} \sum_{t=1}^T y_{it} + \sigma_\alpha^{-2} \mu_\alpha^{(r)}}{\lambda_\alpha} + \frac{z_i^{(r+0.5)}}{\sqrt{\lambda_\alpha}} \\ &\quad - \frac{\sigma_\alpha^{-2} \mu_\alpha^{(r)}}{\lambda_\alpha} - \frac{\sigma_\epsilon^{-2} T \bar{y}_i}{\lambda_\alpha} - \frac{\bar{z}^{(r+0.5)}}{\sqrt{\lambda_\alpha}} - \frac{z_0^{(r+0.5)}}{\sqrt{\lambda_{\mu SA}}} \\ &= \frac{\sigma_\epsilon^{-2} \sum_{t=1}^T (y_{it} - \bar{y}_i)}{\lambda_\alpha} + \frac{z_i^{(r+0.5)} - \bar{z}^{(r+0.5)}}{\sqrt{\lambda_\alpha}} - \frac{z_0^{(r+0.5)}}{\sqrt{\lambda_{\mu SA}}}, \end{aligned} \quad (18)$$

which implies that $\tilde{\alpha}_i^{(r+0.5)}$ does not depend on $\mu_\alpha^{(r)}$. Thus, $\mu_\alpha^{(r+1)}$ in (17) is independent of $\mu_\alpha^{(r)}$.

The AA→SA ASIS algorithm is summarized as follows:

$$\begin{aligned}
\tilde{\alpha}_i^{(r+0.5)} &= \frac{\sigma_\epsilon^{-2} \sum_{t=1}^T (y_{it} - \mu_\alpha^{(r)})}{\lambda_\alpha} + \frac{z_i^{(r+0.5)}}{\sqrt{\lambda_\alpha}}, \\
\mu_\alpha^{(r+0.5)} &= \frac{\sigma_\epsilon^{-2} \sum_{i=1}^N \sum_{t=1}^T (y_{it} - \tilde{\alpha}_i^{(r+0.5)}) + \tau_\alpha^{-2} \varphi_\alpha}{\lambda_{\mu AA}} + \frac{z_0^{(r+0.5)}}{\sqrt{\lambda_{\mu AA}}}, \\
\alpha_i^{(r+0.5)} &= \tilde{\alpha}_i^{(r+0.5)} + \mu_\alpha^{(r+0.5)}, \\
\mu_\alpha^{(r+1)} &= \frac{\sigma_\alpha^{-2} \sum_{i=1}^N \alpha_i^{(r+0.5)} + \tau_\alpha^{-2} \varphi_\alpha}{\lambda_{\mu SA}} + \frac{z_0^{(r+1)}}{\sqrt{\lambda_{\mu SA}}}.
\end{aligned} \tag{19}$$

If the approximation in equation (14) holds, then we have:

$$\begin{aligned}
\alpha_i^{(r+0.5)} &= \tilde{\alpha}_i^{(r+0.5)} + \mu_\alpha^{(r+0.5)} \\
&= \frac{\sigma_\epsilon^{-2} \sum_{t=1}^T (y_{it} - \mu_\alpha^{(r)})}{\lambda_\alpha} + \frac{z_i^{(r+0.5)}}{\sqrt{\lambda_\alpha}} + \frac{\sigma_\epsilon^{-2} T \mu_\alpha^{(r)}}{\lambda_\alpha} + \frac{\sigma_\alpha^{-2} \bar{y}}{\lambda_\alpha} - \frac{\bar{z}^{(r+0.5)}}{\sqrt{\lambda_\alpha}} + \frac{z_0^{(r+0.5)}}{\sqrt{\lambda_{\mu AA}}} \\
&= \bar{y} + \frac{z_i^{(r+0.5)} - \bar{z}^{(r+0.5)}}{\sqrt{\lambda_\alpha}} + \frac{z_0^{(r+0.5)}}{\sqrt{\lambda_{\mu AA}}}.
\end{aligned} \tag{20}$$

As with equation (17), $\mu_\alpha^{(r+1)}$ in equation (19) is independent of $\mu_\alpha^{(r)}$.

Theorem 2. $\{\mu_\alpha^{(r)}\}_{r=1}^R$ generated by SA→AA and AA→SA ASIS algorithms is approximately an independent and identically distributed (IID) sequence.

This theorem follows directly from equations (17) and (19). Furthermore, if $\mu_\alpha^{(r)}$ is approximately IID, then so is $\alpha_i^{(r+0.5)}$. In conclusion, SA→AA and AA→SA ASIS algorithms can generate an approximately IID sequence $\{(\alpha_1^{(r)}, \dots, \alpha_N^{(r)}, \mu_\alpha^{(r)})\}_{r=1}^R$ when the product $\tau_\alpha^2 N$ is sufficiently large. Figure 2 shows that $\mu_\alpha^{(r+1)}$ becomes independent of $\mu_\alpha^{(r)}$ under the ASIS framework. Therein, the solid arrows denote dependency relationships between μ_α and α , whereas the wavy arrows indicate asymptotic independence. The blue boxed segment in Figure 2 highlights a key insight: by generating $\mu_\alpha^{(r+1)}$ via SA and AA steps, $\mu_\alpha^{(r+1)}$ becomes independent of $\mu_\alpha^{(r)}$.

4 Simulation Study

The theoretical results were verified via simulations using synthetic data generated under several scenarios described below. MCMC estimations were conducted across 12 settings for four panel configurations: $(N, T) = (10, 10), (10, 100), (500, 10),$ and $(500, 100)$. These included three patterns: Pattern 1, where SA is expected to converge faster; Pattern 2, where AA is expected to converge faster; and Pattern 3, where SA and AA are expected to exhibit comparable rates. These expectations were based on the relative convergence derived in Corollary 1. Each simulation was run for 10,000 iterations, with a 1,000-iteration burn-in period. The results were averaged over 100 independent MCMC runs. Because the convergence conditions in Corollary 1 depend on the time dimension T , the prior distribution parameters used for each configuration are provided in the footnotes of the corresponding tables.

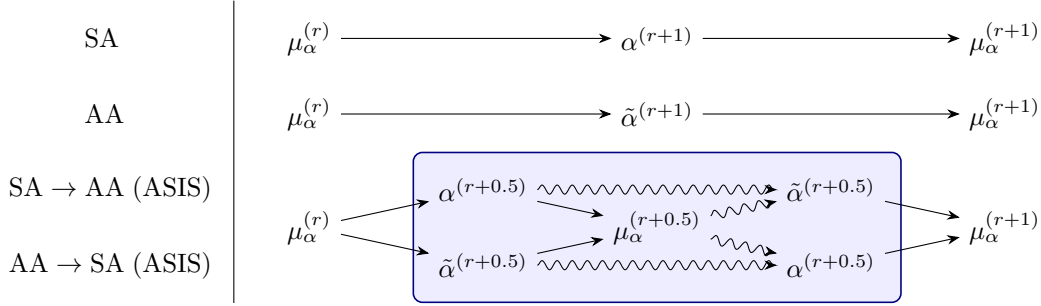


Figure 2: Sampling flow for SA, AA, and ancillarity-sufficiency interweaving strategy (ASIS). In SA and AA, the updated global mean $\mu_\alpha^{(r+1)}$ depends on its previous value $\mu_\alpha^{(r)}$. Contrarily, in ASIS, $\mu_\alpha^{(r+1)}$ is generated independently of $\mu_\alpha^{(r)}$.

In Tables 1 to 4, we compare the Monte Carlo standard errors (MCSEs) of μ_α . ASIS consistently showed the best performance across all settings; however, the primary focus of this study is the MCSE ratio between SA and AA under Patterns 1, 2, and 3. Comparison of Patterns 1 and 2 revealed that SA had consistently lower MCSE than AA in Pattern 1, whereas AA had lower MCSE lower than SA in Pattern 2. These findings matched the predictions of Corollary 1. Under Pattern 3, SA and AA exhibited noticeable MCSE differences when $N = 10$ (Tables 1 and 2). However, for $N = 500$ (Tables 3 and 4), the difference was negligible; these findings also aligned with the theoretical prediction of Corollary 1. Further support for the theoretical findings from Theorems 1 and 2 is provided in Figures 3 to 6, where the autocorrelation function (ACF) of μ_α under ASIS decayed considerably faster than that under SA and AA.

Table 1: MCSE comparison of μ_α ($N = 10, T = 10$)

		SA	AA	ASIS
Pattern 1:	$\sigma_\varepsilon^2 < T\sigma_\alpha^2$	2.980	6.178	2.427
Pattern 2:	$\sigma_\varepsilon^2 > T\sigma_\alpha^2$	56.286	17.057	13.716
Pattern 3:	$\sigma_\varepsilon^2 = T\sigma_\alpha^2$	9.644	14.399	6.697

Boldface denotes the smallest MCSE.

All values are scaled by $\times 10^{-5}$.

Pattern-specific parameter values:

Pattern 1 ($<$) : $(\sigma_\varepsilon, \sigma_\alpha) = (1, 1)$;

Pattern 2 ($>$) : $(\sigma_\varepsilon, \sigma_\alpha) = (10, 1)$;

Pattern 3 ($=$) : $(\sigma_\varepsilon, \sigma_\alpha) = (\sqrt{10}, 1)$.

5 Real Data Analysis

The proposed algorithm was demonstrated on the U.S. “Cigarette” panel dataset, originally compiled by [1] and later popularized by [23]. This dataset covers 48 states over 11 years and is widely used as a standard benchmark for teaching and empirical evaluation in econometrics.

Table 2: MCSE comparison of μ_α ($N = 10, T = 100$)

		SA	AA	ASIS
Pattern 1:	$\sigma_\varepsilon^2 < T\sigma_\alpha^2$	3.255	8.587	2.877
Pattern 2:	$\sigma_\varepsilon^2 > T\sigma_\alpha^2$	53.828	17.665	13.781
Pattern 3:	$\sigma_\varepsilon^2 = T\sigma_\alpha^2$	9.221	13.949	6.589

All values are scaled by $\times 10^{-5}$. Boldface indicates the smallest MCSE. The parameter values for each pattern are as follows:

Pattern 1 ($<$) : $(\sigma_\varepsilon, \sigma_\alpha) = (\sqrt{10}, 1)$;
Pattern 2 ($>$) : $(\sigma_\varepsilon, \sigma_\alpha) = (\sqrt{1000}, 1)$;
Pattern 3 ($=$) : $(\sigma_\varepsilon, \sigma_\alpha) = (10, 1)$.

Table 3: MCSE comparison of μ_α ($N = 500, T = 10$)

		SA	AA	ASIS
Pattern 1:	$\sigma_\varepsilon^2 < T\sigma_\alpha^2$	0.600	2.279	0.567
Pattern 2:	$\sigma_\varepsilon^2 > T\sigma_\alpha^2$	10.496	1.753	1.722
Pattern 3:	$\sigma_\varepsilon^2 = T\sigma_\alpha^2$	1.192	1.126	0.738

Boldface denotes the smallest MCSE.

All values are scaled by $\times 10^{-5}$.

Pattern numbering as in Table 1.

Table 4: MCSE comparison of μ_α ($N = 500, T = 100$)

		SA	AA	ASIS
Pattern 1:	$\sigma_\varepsilon^2 < T\sigma_\alpha^2$	0.618	2.379	0.585
Pattern 2:	$\sigma_\varepsilon^2 > T\sigma_\alpha^2$	8.815	1.813	1.733
Pattern 3:	$\sigma_\varepsilon^2 = T\sigma_\alpha^2$	1.169	1.168	0.744

Boldface denotes the smallest MCSE.

All values are scaled by $\times 10^{-5}$.

Pattern numbering as in Table 2.

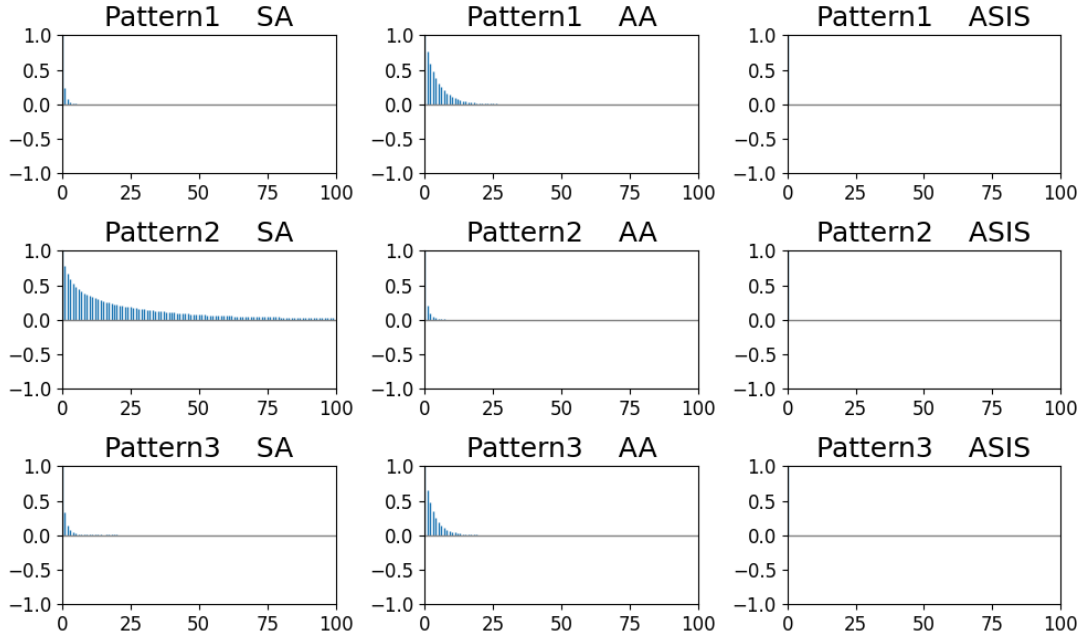


Figure 3: ACF plot of μ_α for $N = 10$ and $T = 10$.

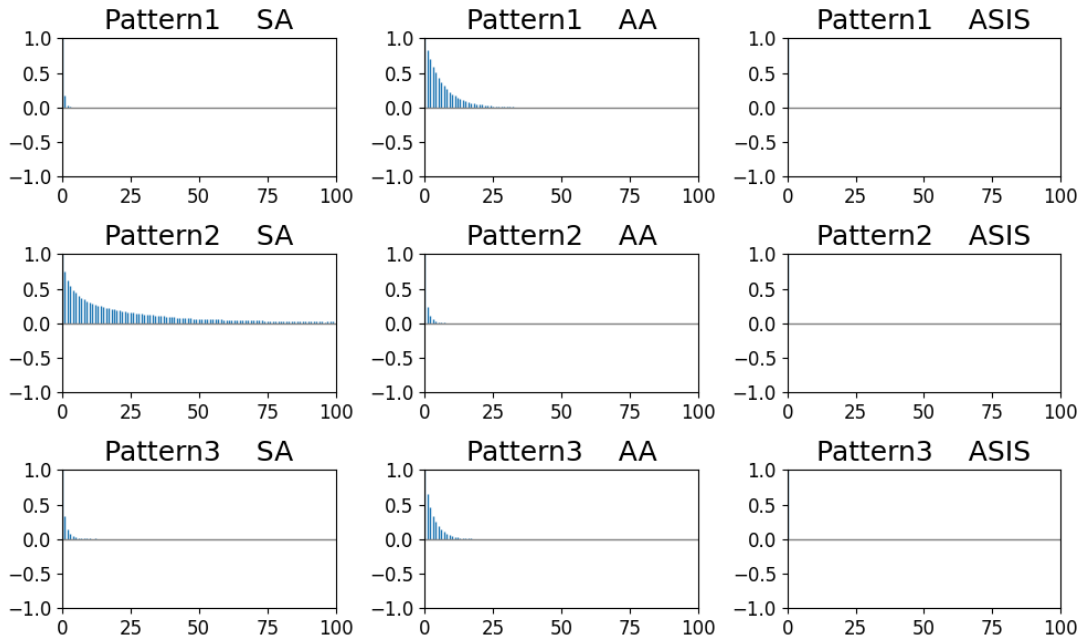


Figure 4: ACF plot of μ_α for $N = 10$ and $T = 100$.

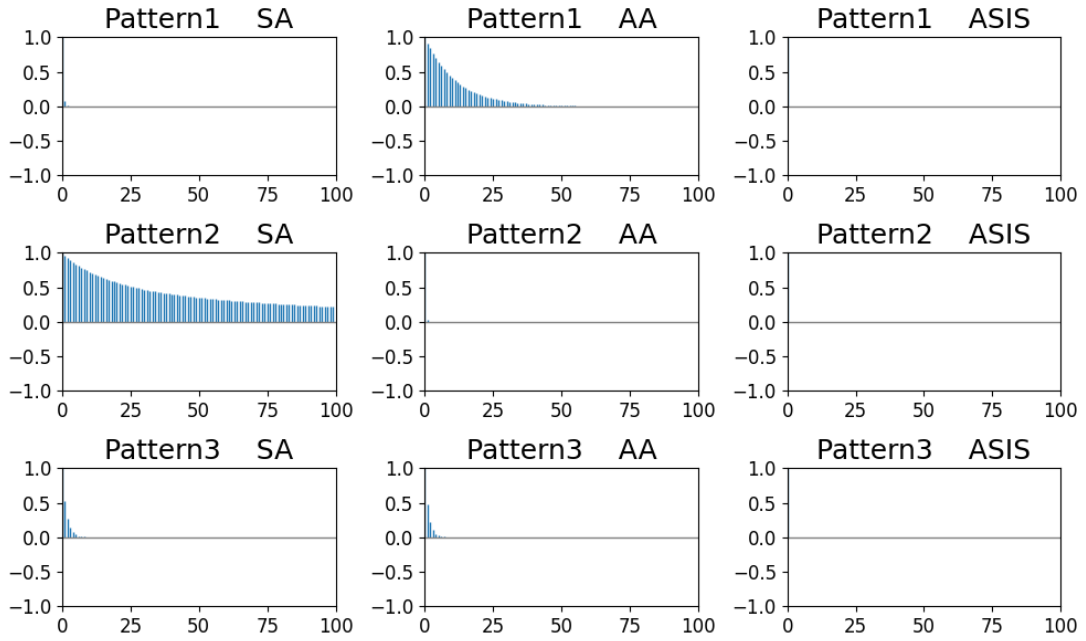


Figure 5: ACF plot of μ_α for $N = 500$ and $T = 10$.

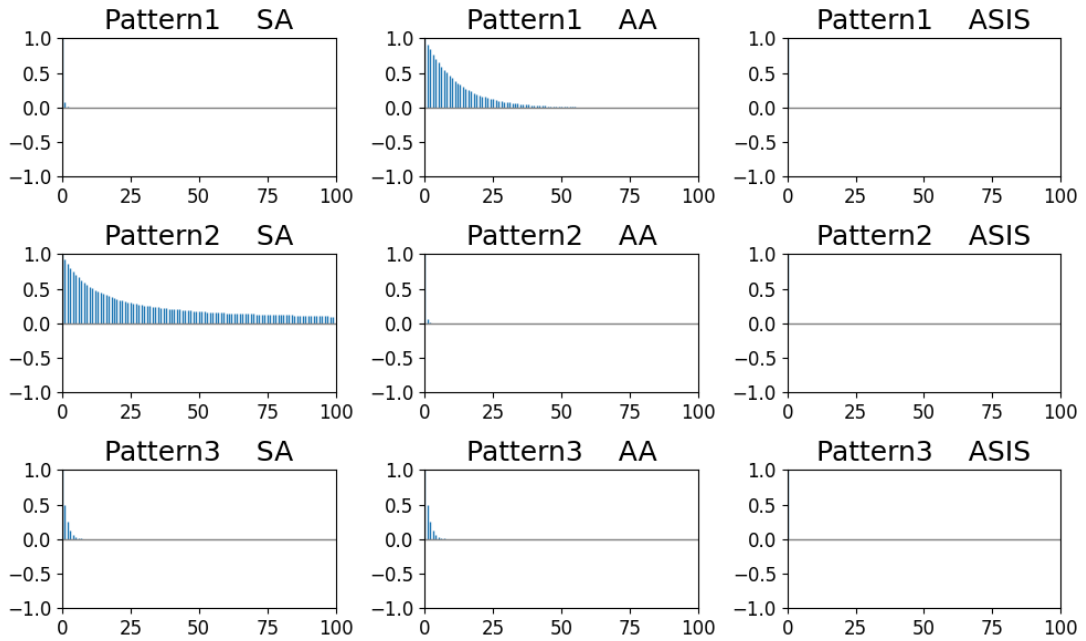


Figure 6: ACF plot of μ_α for $N = 500$ and $T = 100$.

It is widely featured in leading textbooks [11] and instructional materials such as [3], and is readily available in R and Stata, ensuring full replicability. Since benchmark estimates—such as elasticities and other key parameters—are firmly established in the literature, the numerical and computational advantages of the proposed algorithm can be meaningfully assessed against these well-known reference values; this enabled a focused evaluation of the performance of the proposed algorithm.

Following [1, 23], a predictive model was constructed for per capita cigarette pack consumption. As real-world panel datasets almost always include influences beyond individual-specific effects, controlling for observable covariates is essential. Therefore, real per capita income, average retail price per pack (including sales taxes), and average excise tax per pack were included as covariates herein. Following the aforementioned textbook treatments, the baseline specification was extended by incorporating the regressor term $\mathbf{x}_{it}'\beta$. We defined $\tilde{y}_{it} = y_{it} - \mathbf{x}_{it}'\beta$ by partialing out the covariates, thereby recovering a structure with only individual effects for α_i . Thus, the previously established efficiency results remain applicable for this setting.

Figure 7 and Table 5 reports the empirical results. Across ACF and MCSE metrics, ASIS consistently outperforms SA and AA. The lower ACF and MCSE values for ASIS confirm its superior mixing and sampling efficiency on real data, consistent with the improvements observed in the simulation study.

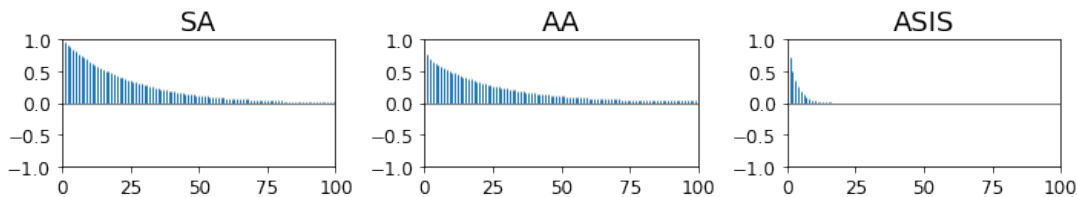


Figure 7: ACF plot of μ_α for the cigarette data.

Table 5: MCSE comparison of μ_α

Method	SA	AA	ASIS
MCSE	8.673	8.232	3.072

Boldface denotes the smallest MCSE.

All values are scaled by $\times 10^{-3}$.

6 Conclusion

This study has advanced Bayesian panel data analysis in three key respects. First, it provides the first rigorous theoretical justification for applying ASIS to hierarchical panel models. The asymptotic theory demonstrates that when the product of the prior variance of the unobserved heterogeneity and N is sufficiently large, the latent individual effects α_i can be sampled almost independently of the global mean μ_α . This decoupling explains why ASIS, already effective in state-space models, continues to mix efficiently in panel settings, highlighting its suitability for modern “tall” datasets.

Second, we introduce clear and easy-to-verify criteria for determining whether SA or AA yields faster geometric convergence. We also show that ASIS, which interweaves SA and AA, renders the sequence $\{\mu_{\alpha}^{(r)}\}_{r=1}^R$ approximately IID and achieves optimal convergence efficiency in all cases.

Third, although the theoretical results are asymptotic, the simulation study confirms that the ordering predicted by Corollary 1 holds even for small panels *e.g.*, $N = 10$. This robustness extends the practical applicability of the method, which has been successfully applied in empirical studies across finance [15], marketing [22], and sports analytics [16].

Regardless, several aspects require further exploration beyond the scope of this study. As the present analysis focused on the simplest baseline specification, incorporating additional regressors or increasingly complex hierarchical structures may influence certain quantitative aspects; however, the qualitative ordering between SA and AA will likely remain robust. Extending the theoretical framework and sampler to nonGaussian panel models, such as panel logit or probit, will substantially enhance their empirical applicability. Finally, many real-world datasets exhibit cross-sectional heterogeneity and rich temporal dynamics. Adapting the proposed approach to time-series hierarchies, especially those common in financial econometrics, is a promising future research direction.

References

- [1] Baltagi, B. H., and Levin, D. 1986. Estimating dynamic demand for cigarettes using panel data: the effects of bootlegging, taxation and advertising reconsidered. *The Review of Economics and Statistics* 148–155.
- [2] Chib, S. 2008. Panel Data Modeling and Inference: A Bayesian Primer. In Mátyás, L., and Sevestre, P., eds., *The Econometrics of Panel Data*, volume 46. Berlin, Heidelberg: Springer Berlin Heidelberg. 479–515.
- [3] Fritsch, M.; Pua, A. A. Y.; and Schnurbus, J. 2024. Teaching advanced topics in econometrics using introductory textbooks: The case of dynamic panel data methods. *International Review of Economics Education* 47:100297.
- [4] Gelfand, A. E.; Sahu, S. K.; and Carlin, B. P. 1995. Efficient parametrisations for normal linear mixed models. *Biometrika* 82(3):479–488.
- [5] Gelfand, A. E.; Sahu, S. K.; and Carlin, B. P. 1996. Efficient parametrizations for generalized linear mixed models,(with discussion).
- [6] Geman, S., and Geman, D. 1984. Stochastic relaxation, gibbs distributions, and the bayesian restoration of images. *IEEE Transactions on pattern analysis and machine intelligence* (6):721–741.
- [7] Hastings, W. K. 1970. Monte carlo sampling methods using markov chains and their applications.
- [8] Hills, S. E., and Smith, A. F. 1992. Parameterization issues in bayesian inference. *Bayesian statistics* 4:227–246.

- [9] Kastner, G., and Frühwirth-Schnatter, S. 2014. Ancillarity-sufficiency interweaving strategy (asis) for boosting mcmc estimation of stochastic volatility models. *Computational Statistics & Data Analysis* 76:408–423.
- [10] Kastner, G.; Frühwirth-Schnatter, S.; and Lopes, H. F. 2017. Efficient bayesian inference for multivariate factor stochastic volatility models. *Journal of Computational and Graphical Statistics* 26(4):905–917.
- [11] Kleibergen, C., and Zeileis, A. 2008. *Applied Econometrics with R*. Use R! New York: Springer.
- [12] Li, M., and Scharth, M. 2020. Leverage, asymmetry, and heavy tails in the high-dimensional factor stochastic volatility model. *Journal of Business & Economic Statistics* 40(1):285–301.
- [13] Li, C.-e., and Shi, J.-h. 2020. Mcmc interweaving strategy for estimating stochastic volatility model and its application. *Communications in Statistics - Simulation and Computation* 52(2):557–568.
- [14] Metropolis, N.; Rosenbluth, A. W.; Rosenbluth, M. N.; Teller, A. H.; and Teller, E. 1953. Equation of state calculations by fast computing machines. *The journal of chemical physics* 21(6):1087–1092.
- [15] Nakakita, M., and Nakatsuma, T. 2021. Bayesian analysis of intraday stochastic volatility models of high-frequency stock returns with skew heavy-tailed errors. *Journal of Risk and Financial Management* 14(4):145.
- [16] Nakakita, M., and Nakatsuma, T. 2023. Hierarchical bayesian analysis of racehorse running ability and jockey skills. *International Journal of Computer Science in Sport* 22(2):1–25.
- [17] Nakakita, M., and Nakatsuma, T. 2024. A hierarchical bayesian approach for identifying socioeconomic factors influencing self-rated health in japan. *Healthcare Analytics* 6:100367.
- [18] Nakakita, M., and Nakatsuma, T. 2025. Analysis of the trading interval duration for the bitcoin market using high-frequency transaction data. *Quantitative Finance and Economics* 9(1):202–241.
- [19] Papaspiliopoulos, O.; Roberts, G. O.; and Sköld, M. 2003. Non-centered parameterisations for hierarchical models and data augmentation. *Bayesian statistics* 7:307–326.
- [20] Papaspiliopoulos, O.; Roberts, G. O.; and Sköld, M. 2007. A general framework for the parametrization of hierarchical models. *Statistical Science* 59–73.
- [21] Roberts, G. O., and Sahu, S. K. 1997. Updating schemes, correlation structure, blocking and parameterization for the gibbs sampler. *Journal of the Royal Statistical Society Series B: Statistical Methodology* 59(2):291–317.
- [22] Saito, W.; Nakakita, M.; and Nakatsuma, T. 2024. Comparative analysis of japanese rice wine export trends: Large firms in the nada region vs. smes in other regions. *World* 5(3):700–722.
- [23] Stock, J., and Watson, M. 2003. *Introduction to Econometrics*. Addison-Wesley series in economics. Addison Wesley.

- [24] Tanner, M. A., and Wong, W. H. 1987. The Calculation of Posterior Distributions by Data Augmentation. *Journal of the American Statistical Association* 82(398):528–540.
- [25] Toyabe, T.; Nakakita, M.; and Nakatsuma, T. 2024. Bayesian analysis of stochastic conditional duration models with intraday and intra-deferred future seasonalities in high-frequency commodity market. In *2024 16th IIAI International Congress on Advanced Applied Informatics (IIAI-AAI)*, 305–311.
- [26] Xu, X.; Meng, X.-L.; and Yu, Y. 2013. Thank god that regressing y on x is not the same as regressing x on y: Direct and indirect residual augmentations. *Journal of Computational and Graphical Statistics* 22(3):598–622.
- [27] Yu, Y., and Meng, X.-L. 2011. To Center or Not to Center: That Is Not the Question—An Ancillarity–Sufficiency Interweaving Strategy (ASIS) for Boosting MCMC Efficiency. *Journal of Computational and Graphical Statistics* 20(3):531–570.